

# Solid Dispersion of Curcumin as Polymeric Films for Bioenhancement and Improved Therapy of Rheumatoid Arthritis

Prashant P. Mande<sup>1</sup> · Sagar S. Bachhav<sup>1</sup> · Padma V. Devarajan<sup>1</sup>

Received: 14 January 2016 / Accepted: 27 April 2016 / Published online: 31 May 2016  
© Springer Science+Business Media New York 2016

## ABSTRACT

**Purpose** The aim of our study was development of advanced third generation Curcumin self microemulsifying composition solid dispersion (Cur SMEC-SD) with high drug loading, improved stability, rapid *in-vitro* dissolution and enhanced bioavailability for improved therapy of rheumatoid arthritis.

**Method** The Cur SMEC-SD comprising polymers (KollidonVA64[KVA], Eudragits, HPMC and Soluplus) and self microemulsifying composition of surfactant:co-surfactant:oil were coated onto rapidly disintegrating inert tablet core. SDs evaluated for stability, *in-vitro* release and bioenhancement.

**Results** Cur SMEC-SDs exhibited high Cur loading of 45% w/w and microemulsion formation with globule size (~100 nm) irrespective of polymers. Among the polymers, SD with KVA revealed exceptionally low contact angle (7°C) and rapid *in-vitro* release ( $t_{50\%}$ -6.45 min). No crystallization was evident as confirmed by SEM, DSC and XRD and is attributed to SMEC aided solubilization/amorphisation, and interaction of KVA with Cur seen in the FTIR spectra. Stability was confirmed as per ICH guidelines. Remarkable bioenhancement with Cur SMEC-SD was confirmed by the > four fold and a two fold compared to Cur and Cur-SD without SMEC respectively. High efficacy ~80% compared to Indomethacin, seen with rheumatoid arthritis (RA) induced rats coupled with no adverse toxicity.

**Conclusion** The advanced third generation Cur SMEC-SD presents a practical technological advancement and suggests Cur SMEC-SD as promising alternative for RA therapy.

**KEY WORDS** curcumin · SMEC · advanced third generation SD · bioavailability · rheumatoid arthritis

## ABBREVIATIONS

CFA	Complete Freund's adjuvant
Cur	Curcumin
DSC	Differential scanning calorimetric
KVA	Kollidon VA 64
C <sub>max</sub>	Peak drug concentration
RBC	Red blood cells
RF	Rheumatoid factor
SEM	Scanning electron microscopy
SMEC	Self-microemulsifying composition
CRP	Serum C reactive protein
SD	Solid dispersion
WBC	White blood cells
XRD	X ray powder diffraction

## INTRODUCTION

Curcumin (Cur), a natural safe polyphenol, because of its significant anti-inflammatory and anti-oxidant properties has demonstrated its usefulness in wide variety of diseases (1). However poor aqueous solubility of Cur continues to be one of the biggest challenges in pharmaceutical development (2). A number of approaches have been evaluated to enhance dissolution rate and bioavailability of Cur including complexation (3), micelles (4) microemulsion (5) solid-lipid nanoparticles (6) and solid dispersions (SD) (7). Although SD continues to be a

✉ Padma V. Devarajan  
pvdevarajan@gmail.com

<sup>1</sup> Department of Pharmaceutical Sciences and Technology, Institute of Chemical Technology, N. P. Marg, Matunga (E), Mumbai, Maharashtra, India

promising strategy for bioenhancement of drug candidates (8), limited physical stability and thereby restricted drug loading pose constraints. These limitations have been addressed through development of third generation SDs which comprise polymers in combination with surfactants which significantly decrease drug crystallization to enhance stability (9). The superiority of third generation SDs was clearly evident when the third generation SDs were compared with first generation solid dispersions which comprise small molecule crystalline carriers and second generation SD which comprise amorphous carriers usually polymers (10). A third generation felodipine SD containing HPMC as carrier and poloxamer as surfactant exhibited suppressed crystallization of the drug (11). SDs of LAB68 in a polymeric carrier exhibited high physical stability, improved dissolution rate and enhanced bioavailability when combined with combinations of surfactants (polysorbate 80) and solubilizers (PEG) (12). Self-emulsifying components like Pluronic F-68 enhanced dispersibility in the carrier and also improved aqueous solubility of poorly water soluble diacerein (13). Third generation SDs of ferulic acid embedded in electrospun nanofibers enabled high dissolution rate (14). The surfactants in the third generation SDs provided an additional advantage of surfactant imparted self-emulsifying properties which facilitated the added advantage of bioenhancement (15).

Bioenhancement of poorly soluble drugs from self-microemulsifying composition (SMEC) is well reported and superior to self-emulsifying compositions (16). We therefore replaced the surfactant with a self-microemulsifying composition (SMEC) and also exploited the film forming property of the polymer to design advanced third generation SDs as films. The increased surface area together with the hydrophilicity and solubilizing capacity of the SMEC comprising surfactant, solubiliser/co-surfactants and oil could provide the advantages of enhanced physical stability, rapid release and also bioenhancement, an important need for Cur. The aim of our study included the development of advanced third generation Cur SMEC-SDs with the objectives of high drug loading, improved stability, rapid *in-vitro* dissolution rate and enhanced bioavailability. We also demonstrate promise of the Cur SMEC-SD for therapy of rheumatoid arthritis in the Complete Freund's Adjuvant (CFA) arthritis model in rats. Rheumatoid arthritis was selected as the disease model as it is a debilitating disease wherein safer alternatives to conventional therapy are a dire need.

## MATERIALS AND METHOD

### Materials

Curcumin (Konark Herbals & Health Care, India), Capmul MCM and Captex 300 oil (Abitec Corporation India),

Labrasol (Gattefosse, France), Eudragit EPO and Eudragit RLPO, Aerosil 200, Indomethacin (Evonik India pvt ltd), Kollidon VA 64 (KVA), Soluplus (BASF India) and Hydroxypropyl methylcellulose (Methocel HPMC E5; Colorcon), Acetonitrile HPLC grade (Azeocryst Organics, India) were kindly supplied as gift samples. Tween 80 (Merck India), propylene glycol (Merck India), Magnesium Stearate (Signet chemicals Co Pvt Ltd), MCC 102 (FMC Pvt. Ltd), Lactose - Supertab 11 (FMC Pvt. Ltd), Complete Freund's Adjuvant (Sigma Aldrich, USA), Serum C reactive protein (CRP) kit (Lab Care Diagnostics India Pvt. Ltd.), Acetone AR grade (S. D. fine chemicals) and Methanol HPLC grade (S. D. fine chemicals) were procured from respective manufacturer.

### Formulation of Self Microemulsifying Composition (SMEC)

#### Solubility of Cur

The solubility of Cur in various oils (Capmul MCM, Captex 300), surfactants (Tween 80, Labrasol), and co-surfactants (Propylene glycol) was determined by the shake flask method. Excess Cur was added to 1.5 mL micro centrifuge tube containing 1 mL of the excipient and the mixture vortexed for 10 min. Following agitation in a shaker water bath maintained at 28°C for 24 h, the samples were centrifuged at 5000 rpm for 15 min (Hermle, USA) and the supernatant was analysed by UV spectrophotometry at 425 nm.

#### Construction of Pseudo-Ternary Phase Diagrams

Pseudo-ternary phase diagrams were constructed using the water titration method (17), with Capmul MCM and Captex 300 as oil phase, tween 80 (T80) and labrasol as surfactants (S) and propylene glycol (PG) as co-surfactant (CoS). Mixtures of S/CoS (2:1) with oils were prepared in the ratios 9:1, 8:2, 7:3, 6:4, 5:5, 4:6, 3:7, 2:8 to 1:9. Each mixture was slowly titrated with aliquots of distilled water and stirred at room temperature to attain equilibrium. After equilibrium, the samples were visually checked using an optical polariser. Clear and isotropic samples were deemed to be within the microemulsion region. Based on the results, appropriate percentage of oil, surfactant and co-surfactant were selected, correlated in the phase diagram and used for preparation of SMEC.

#### Preparation of SMEC

Oil (Capmul MCM - 20% w/w), surfactant (Tween 80–54% w/w) and co-surfactant (PEG - 26% w/w) were vortex mixed at room temperature to obtain clear and transparent SMEC. Blank SMEC formulation following dilution with water (1:10

and 1:100) were evaluated for globule size and polydispersity index (PDI) using N4 plus submicron particle size analyzer (Beckman Coulter) at 25°C. Solubility of Cur in 1 mL of SMEC was determined by addition of excess Cur till no more dissolved then vortexed and allowed to stand for 24 h. To determine solubility, SMEC were centrifuged at 2000 rpm for 5 min and the supernatant evaluated for Cur by UV spectrophotometer at 425 nm. Solubility of Cur was also evaluated in the S/CoS mixture without the oil.

### Preparation of Coating Solution

The polymers KVA, HPMC, Soluplus, Eudragit EPO and Eudragit RLPO (3% w/v) and SMEC (0.6% w/v) were dissolved in a solvent system comprising acetone: water (80:20) using an overhead stirrer for half an hour. In case of HPMC, the polymer was dispersed in about 20% of required acetone using an overhead stirrer followed by slow addition of water to solubilize HPMC. The remaining acetone was added and the solution mixed until clear. Solubility of Cur in the polymeric solutions (1 mL) was determined by addition of Cur in incremental quantity till no more dissolved. Coating solutions were vortexed and allowed to stand for 10 min, centrifuged at 5000 rpm for 5 min and the supernatant evaluated for Cur by UV spectrophotometer at 425 nm using appropriate blank. Based on the solubility of Cur, solutions comprising polymer 1.5% w/v, SMEC 0.3 and Cur 1.5% w/v were used for coating. A coating solution without SMEC was also evaluated.

### Free Film Study

Free films were obtained by standard casting technique on glass slides (18). The films were observed under a fluorescence microscope using IF550 filter at 4x/0.13PhL lens (Olympus, Japan) for appearance and crystallization of Cur and images captured using digital camera.

### Preparation of Cur SMEC-SDs Loaded Tablets

Cur solid dispersions as films were prepared by dissolving polymer, SMEC and Cur in acetone: H<sub>2</sub>O (80:20) and removal of the solvent following spraying of the solution on inert tablet cores. This enabled deposition of SDs as polymeric films on the tablet cores. Films comprising SMEC results in formation of Cur SMEC-SDs and films without SMEC results Cur SDs. Inert core tablets comprising MCC 102 (49.5% w/w), Supertab 11 (49.5% w/w), Aerosil 200 (0.5% w/w) and magnesium stearate (0.5% w/w), were obtained by direct compression on a 16 station rotary tablet press. The excipients were mixed in a double cone blender (Shreeji Automachine, India) and compressed to tablets of ~250 mg using standard concave punches of 10 mm diameter. SD equivalent to approximately ~30 mg of Cur/tablet could be readily coated.

The coating parameters are shown in Table I. The SD variables evaluated included polymer type [KVA (KSM20), HPMC (HSM20), Soluplus (SSM20), Eudragit EPO (EPSM20) and Eudragit RLPO (RLSM20)] where the number indicates the SMEC concentration in the SD as %w/w, and SMEC concentration in KVA as polymer (KSM0, KSM10, KSM20 and KSM30). A barrier coat of HPMC 3%w/w was coated on the SDs by spraying HPMC (10%w/v) in acetone: water (80:20).

### Differential Scanning Calorimetric (DSC) Study

Plain Cur, plain polymers, Cur SMEC-SDs and Cur SD (~5 mg) were taken in aluminum pans, sealed and subjected to differential scanning calorimetry under nitrogen flow using a Perkin Elmer Pyris 6 DSC thermal analysis instrument. Each sample was heated from 40 to 300°C at a rate of 10°C min<sup>-1</sup>. Empty aluminum pan served as the reference.

### X ray Powder Diffraction (XRD) Study

XRD spectra of the Plain Cur, plain polymer (KVA), Cur SMEC-SDs and Cur SD were recorded at room temperature using Philips Pro Expert diffractometer, with nickel filtered Cu K $\alpha$  radiation at a voltage of 3 kV, 5 mA Current, 4°/min scanning speed, and 5°–70° (2 $\theta$ ) range.

### Fourier Transform Infrared (FTIR) Spectral Study

FTIR spectra of the plain Cur, plain polymers, Cur SMEC-SDs and Cur SD were recorded on an infrared spectrometer (Perkin Elmer, Model spectrum RX) using the KBr pressed disc method. The scanning range was 400–4000 cm<sup>-1</sup>.

### Physicochemical Characterization of Tablets

Tablets were evaluated for assay, disintegration test, hardness and friability following standard methodology. Drug content was analyzed by HPLC using mobile phase comprised of 50 mM sodium dihydrogen orthophosphate buffer (pH 3.0):

**Table I** Operational Parameters for Coating

Parameter	Coating parameters
Coating pan diameter (inch)	12
Batch size (g)	200
Inlet temperature (°C)	40–41
Outlet temperature (°C)	35–37
Atomizing air (bar)	1
Spray rate (g/min)	1–3
Pan speed (RPM)	6–7

acetonitrile (47:53) at a flow rate 1.2 mL/min at 425 nm. HPLC analysis was performed on Jasco LC900 system equipped with Jasco PU-980 Intelligent HPLC pump, Jasco UV-975 Intelligent UV/VIS detector.

### Scanning Electron Microscopy (SEM)

A tablet was mounted on the sample holder (stub) and sputtered with platinum using an auto fine coater and SEM micrographs of the tablets were photographed using a LV-SEM 5800 (JEOL, Japan) at an accelerating voltage of 10 kV.

### Contact Angle Measurement

A drop of distilled water was carefully placed on the tablet surface and the contact angle was measured using a contact angle apparatus (DSA-100, Krüss, Germany) (19).

### Film and Microemulsion Formation

Cur SMEC-SDs and Cur SDs loaded tablets were placed in 200 ml of distilled water at room temperature ( $\sim 28^\circ\text{C}$ ) and evaluated for release of the SD film. Further the samples were subjected to mild agitation, filtered through a  $0.45\ \mu\text{m}$  membrane filter and the average droplet size and polydispersity index (PDI) determined to confirm formation of microemulsion. Size was determined by photon correlation spectroscopy using N4 plus submicron particle size analyzer (Beckman Coulter) at  $25^\circ\text{C}$ .

### In Vitro Drug Release

*In vitro* dissolution of the Cur SMEC-SDs and Cur SD was evaluated on the USP Type II apparatus, at  $37 \pm 0.5^\circ\text{C}$  and 50 rpm paddle speed in 900 ml of simulated gastric fluid (SGF, pH 1.2) without pepsin as dissolution medium. Plain Cur powder was used as reference. Samples (10 ml) were withdrawn at predetermined intervals up to 120 min and analyzed by UV spectrophotometry at 425 nm. Percent cumulative drug release *versus* time profiles were plotted. At the end of dissolution study filtered dissolution samples were also evaluated for average globule size and polydispersity index (PDI) by photon correlation spectroscopy using N4 plus submicron particle size analyzer (Beckman Coulter) at  $25^\circ\text{C}$  (20). Data was analyzed using various kinetic models (21).

### Stability Studies

Cur SMEC-SD (KSM20) was evaluated for stability as per ICH guidelines. Tablets were packed in HDPE containers and stored at intermediate conditions [ $30 \pm 2^\circ\text{C}$ ,  $65 \pm 5\%$  RH] for 3, 6, 9 and 12 months and at accelerated conditions [ $40 \pm 2^\circ\text{C}$ ,  $75 \pm 5\%$  RH] for 3, 6 and 12 months and

evaluated for drug content and drug release. Tablets were also dispersed in water and filtered samples evaluated for globule size of microemulsion.

### In-Vivo Pharmacokinetics and Pharmacodynamic Studies

#### Animals

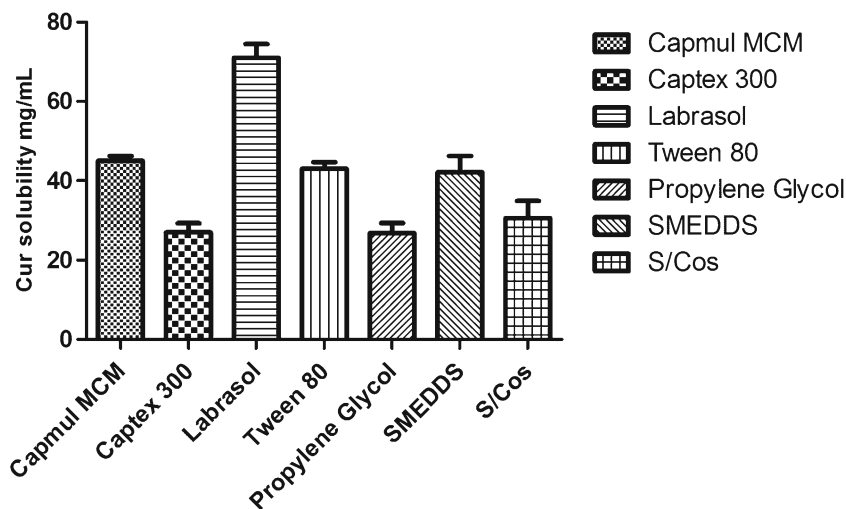
Adult male wistar rats ( $200 \pm 20\ \text{g}$ ) were procured from Haffkine Bio-Pharmaceuticals, Mumbai, India. The rats were housed in groups of six in polypropylene cages at an ambient temperature of  $25 \pm 1^\circ\text{C}$  and 45–55% RH, with a 12 h light/dark cycle. Standard rat chow pellets and water were allowed *ad libitum*. All the experimental procedures were approved by Institutional Animal Ethics Committee (IAEC) of Institute of Chemical Technology, Mumbai (87/1999/CPCSEA) and conducted as per the guidelines of Committee for the Purpose of Control and Supervision of Experiments on Animals (CPCSEA).

#### Bioavailability Study

The rats were divided into three groups ( $n = 12$ ) and were fasted for 8 h prior to the commencement of the study. The rats were administered with Cur suspension in 0.5% carboxymethylcellulose (CMC) (group I), Cur SMEC-SDs (KSM20), Cur SD (KSM0) dispersed in water, at a dose of 50 mg/kg body weight (20) by oral gavage. Animals were anesthetized using a combination of halothane and oxygen and blood samples (0.5 ml) were collected from retro-orbital plexus region with a glass capillary at 0.25, 0.5, 1, 2, 4, 8, 12, 18 and 24 h post dosing into heparinized micro centrifuge tubes ( $n = 4$  per time point). The samples were centrifuged at 10,000 rpm,  $20^\circ\text{C}$  for 10 min and plasma samples separated were stored at  $-70^\circ\text{C}$  until analyzed by HPLC. To 200  $\mu\text{L}$  plasma, 500  $\mu\text{L}$  of acetonitrile was added, vortex mixed and sonicated for 5 min each, followed by centrifugation at 15,000 rpm,  $20^\circ\text{C}$  for 20 min. The supernatant (100  $\mu\text{L}$ ) was assayed using HPLC (Jasco LC 1500) coupled with UV detector (Jasco UV/VIS 1570/1575) at a  $\lambda_{\text{max}}$  of 425 nm. Chromatography was performed on a Spherisorb®C18 column ODS2 ( $5\ \mu\text{m}$ ,  $4.6 \times 250\ \text{mm}$ , Waters, USA) at room temperature under isocratic condition comprised of Acetonitrile: 2% glacial acetic acid pH 3.0 (50:50) at a flow rate of 1.0 mL/min. The recovery of Cur was  $>95\%$  in the developed method indicating suitability of bioanalytical method for plasma analysis. Plasma Cur concentration Vs time curve was plotted and pharmacokinetic parameters were calculated using Non Compartmental Analysis model (Phoenix WinNonlin® software, USA).



**Fig. 1** Solubility of Cur in various components.



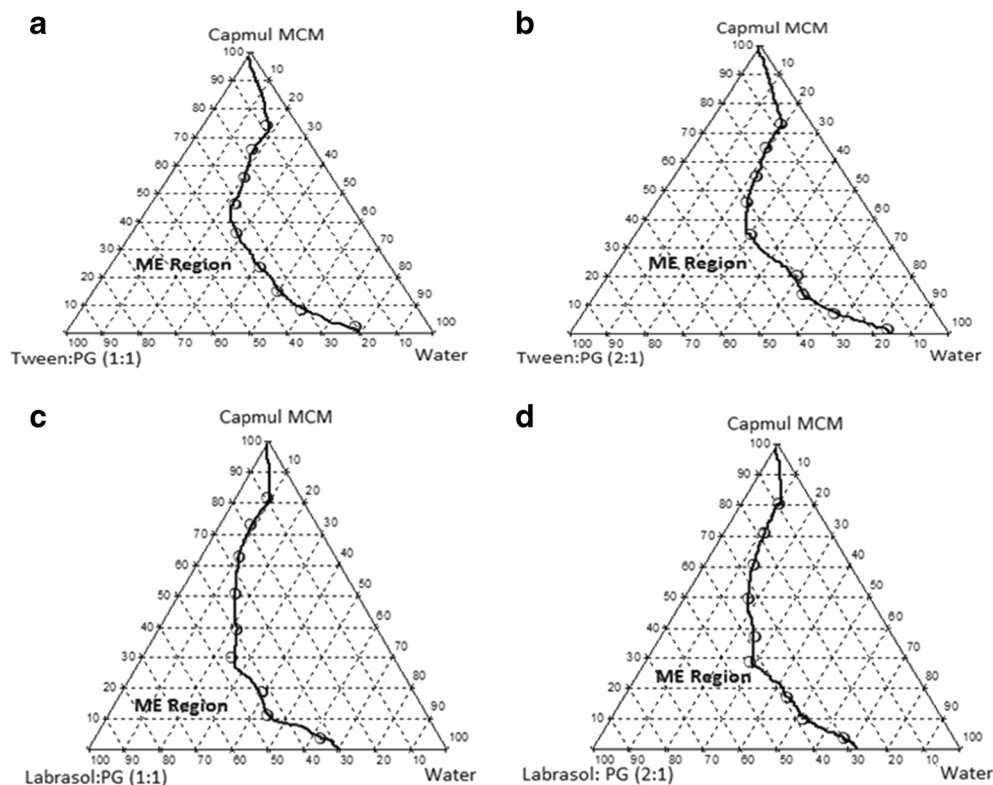
**Anti-Arthritic Activity**

Animals were randomly distributed into six groups with six rats in each group. The left and right hind paw volumes were measured using a digital Plethysmometer 7140 (UgoBasile, Milan, Italy). Arthritis was induced by single intraplantar injection of 0.1 ml of Complete Freund’s Adjuvant (CFA) in the left hind paw of animals in Group II-VI under isoflurane anaesthesia (22). Group I served as the normal control (sham control) and was injected normal saline (0.1 mL). Group II served as CFA control (arthritic control) and was orally

administered 2 mL 0.5% w/v CMC in water by oral gavage daily for 21 days. Group III received Indomethacin (IND) aqueous suspension in 0.5% w/v CMC (10 mg/Kg/day), while Groups IV-VI received Cur (30 mg/Kg/day) as Cur aqueous suspension in 0.5% w/v CMC, Cur SD (KSM0) dispersed in water, Cur SMEC-SD (KSM20) dispersed in water respectively by oral gavage for 21 days.

The volume of the injected and non-injected hind paws and body weight were measured on days 7, 14, and 21. On day 21, blood was collected from retro orbital plexus in two parts, in heparinized tubes for RBC, WBC and Hb estimation

**Fig. 2** Pseudo-ternary phase diagrams of (a) Capmul-T80:PG(1:1) (b) Capmul-T80:PG(2:1) (c) Capmul-Labrasol:PG(1:1) (d) Capmul-Labrasol:PG(2:1).



and non-heparinized tubes for serum collection to monitor serum C - reactive protein (CRP) and serum rheumatoid factor (RF). WBC, RBC and hemoglobin were evaluated using routine laboratory methods and CRP and RF using commercially available kits. Radiographs of the paws acquired on a digital Kodak instrument (Eastman Kodak company, USA), were monitored for soft tissue swelling, narrowing of the joint space, bone density, destruction and enlargement of bone. Rats were then sacrificed with excess of CO<sub>2</sub>. The spleen and thymus were excised and weighed. The liver and synovial joints were excised and fixed in formalin (10%) for histopathological assessment.

### Statistical Analysis

The data are expressed as the mean  $\pm$  SEM. The statistical significance of the difference in each parameter among the groups was evaluated using one-way analysis of variance (ANOVA) followed by Bonferroni as a post-ANOVA test. Criterion for statistically significant difference was chosen to be at  $p < 0.05$ .

## RESULTS AND DISCUSSION

The advanced third generation SDs relied on a combination of polymers with SMEC for bioenhancement. SMEC therefore constituted an integral component and was selected based on solubility of Cur in SMEC components and good self microemulsification property, even at high dilution.

### Selection of SMEC

#### Solubility Study

Cur exhibited good solubility of greater than 25 mg/mL in all components with maximum solubility in labrasol (Fig. 1). Hence all components were considered for construction of pseudoternary phase diagrams. The high solubility seen in labrasol is attributed to formation of hydrogen bond of hydroxyl group in Cur with the polyethylene oxide (PEO) groups of labrasol (23).

#### Pseudo-Ternary Phase Diagrams

Pseudo-ternary phase diagrams constructed to identify the microemulsion regions are depicted in Fig. 2. Capmul MCM a mixture of medium chain mono and diglyceride which is easily emulsified compared to Captex 300 a medium chain triglyceride, revealed larger microemulsion region. Among the surfactants microemulsion regions were significantly larger with T80 than labrasol irrespective of oil.

Further an increase in the microemulsion region with increase in the amount of T80 in S/CoS mixture from 1:1 to 2:1 reflected enhanced solubilisation of the oil and surface wetting property. Additionally the good solubility of Cur in T80 and the well reported ability of T80 to reduce the interfacial tension and also enhance penetration of drug through epithelial cells (20) played an important role in selection of T80 as the surfactant. A S/CoS mixture of T80: PG (2:1) with S/CoS to oil (Capmul MCM) ratio (8:2) corresponding to a system which could be readily diluted with water to form a microemulsion, was chosen as the SMEC.

### Evaluation of SMEC

Globule size after microemulsification is an important characteristic that influences drug release and absorption. The average size of  $114.45 \pm 0.6$  and  $107.56 \pm 0.4$  nm at 1:10 and 1:100 dilution respectively confirmed microemulsion formation even at high dilution. Cur exhibited a high solubility of 42.14 mg/mL in the

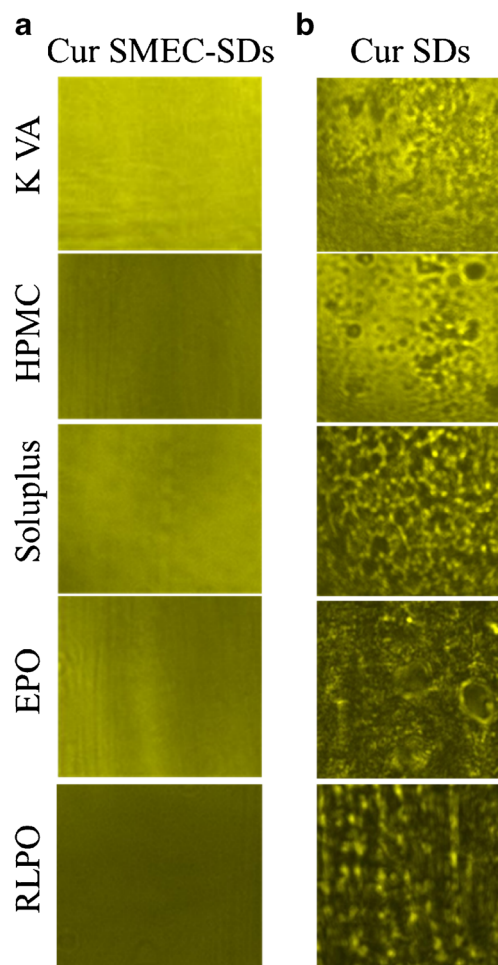


**Fig. 3** Fluorescent micrographs of Cur loaded polymeric films (a) Cur SMEC SDs films and (b) Cur SDs films.

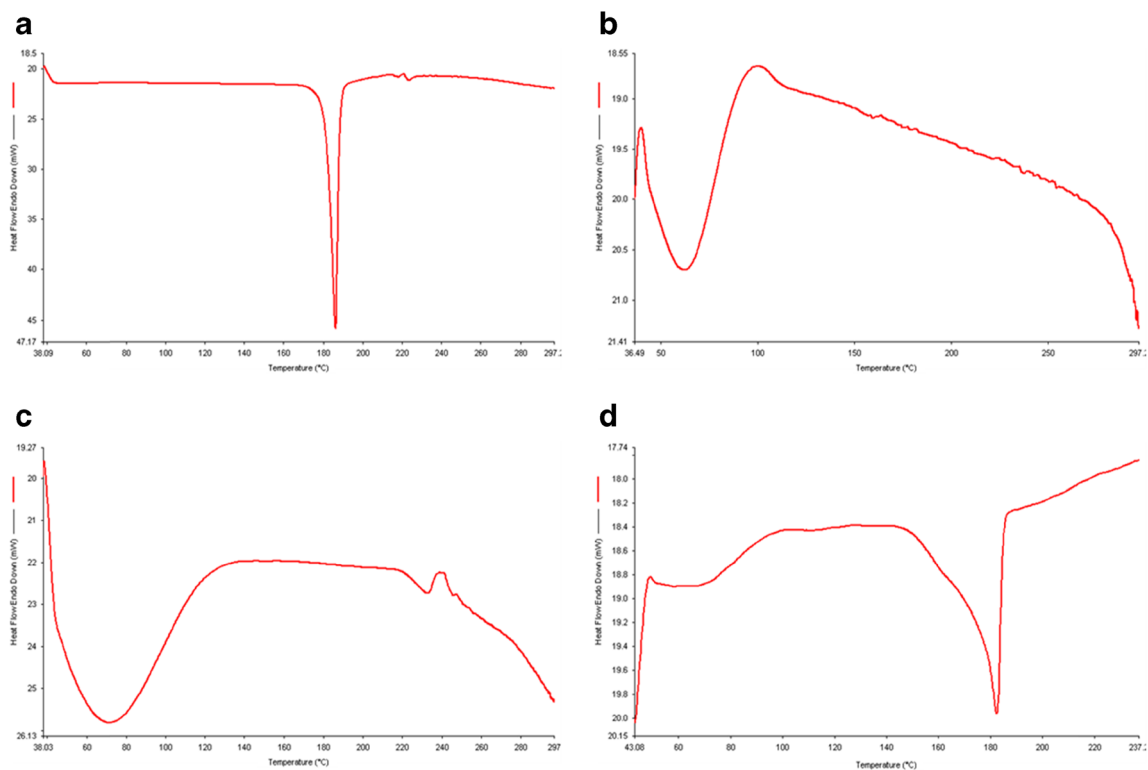


**Fig. 4** DSC profile of (a) Plain Cur (b) KVA (c) KVA Cur SD (KSM0) (d) KVA Cur SMEC-SDs (KSM20) (e) HPMC (f) HPMC Cur SMEC-SDs (HSM20) (g) Eudragit EPO Cur SMEC-SDs (EPSM20) (h) Eudragit RLPO (i) Soluplus (j) Soluplus Cur SMEC-SDs (SSM20) (k) Eudragit RLPO Cur SMEC-SDs (RLSM20).

SMEC. The significantly lower solubility of Cur (29.78 mg/mL) in the S/CoS mixture confirmed the

superior solubilisation capacity of the SMEC. SDs with only S/CoS was therefore not evaluated.

**Fig. 5** Powder X-ray diffraction patterns of (a) Plain Cur (b) KVA (c) KVA Cur SMEC-SDs (KSM20) (d) KVA Cur SDs (KSM0).

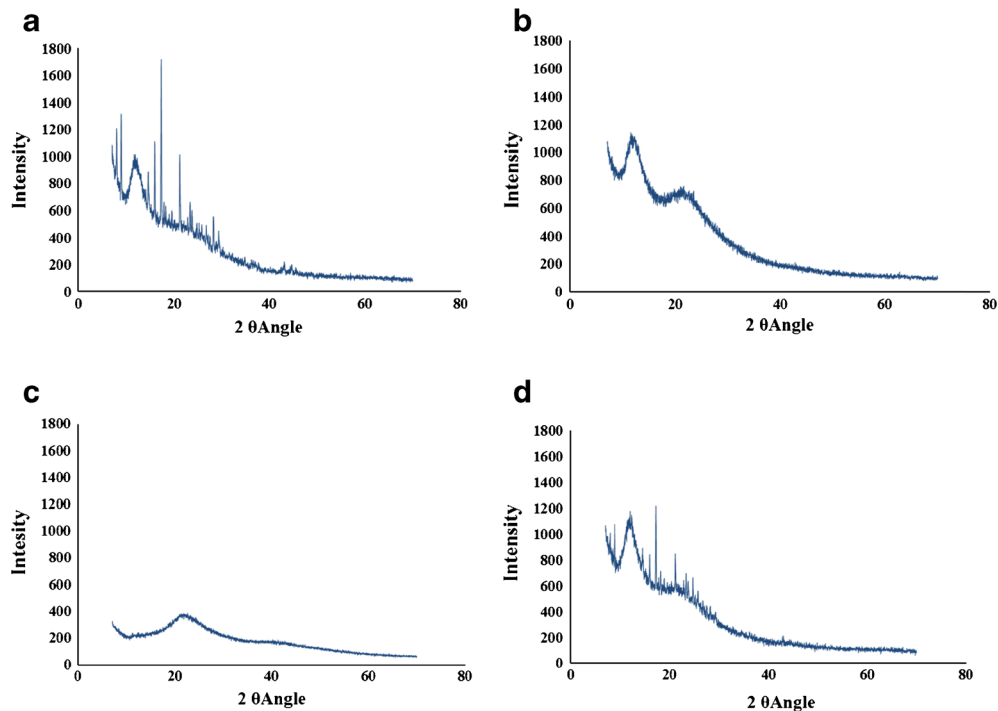
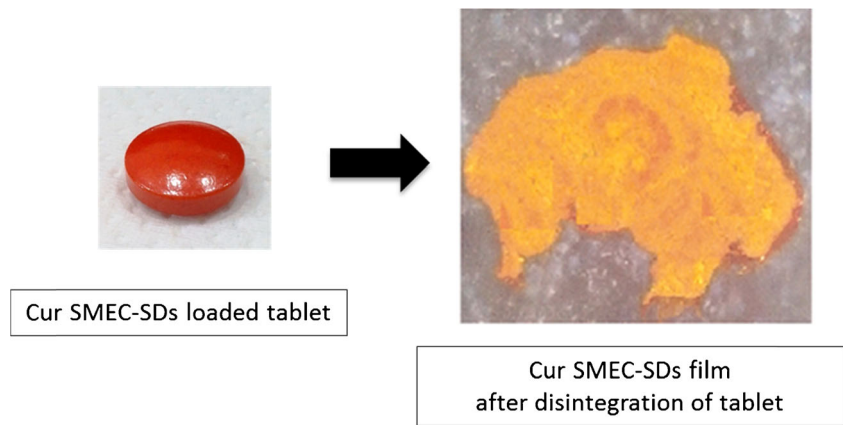


**Fig. 6** Cur SMEC-SDs films released following disintegration of the inert core tablets.



### Free Film Study

This study was undertaken to assess the ability of the SD to form films and retain the drug without crystallization. The saturation solubility of Cur in all the polymeric solutions was comparable ( $P > 0.05$ ) [Cur SMEC-SDs: KVA (27.34 mg/mL), EPO (25.70 mg/mL), Soluplus (24.30 mg/ml), HPMC (23.00 mg/mL), RLPO (22.18 mg/mL) and Cur SD:KVA (16.52 mg/mL)]. SDs were evaluated for film formation and drug stability at a concentration of 15 mg/mL of Cur, which was lower than the saturation concentration observed. All the Cur SMEC-SDs revealed good film formation and none revealed crystallization even after 72 h, as seen from the fluorescence photomicrographs (Fig. 3). Although the Cur SDs exhibited film formation, the appearance of Cur crystals in less than 12 h when observed under a fluorescence microscope, suggested severe physical instability, thereby confirming the promise of the advanced third generation SD comprising SMEC to retard crystallization and enhance stability.

### Differential Scanning Calorimetric (DSC) and X-Ray Powder Diffraction (XRD) Study

A sharp endotherm of Cur at 185°C corresponding to its melting point was evident in the DSC thermogram of Cur and Cur SD (KSM0). Absence of the endotherm in the Cur

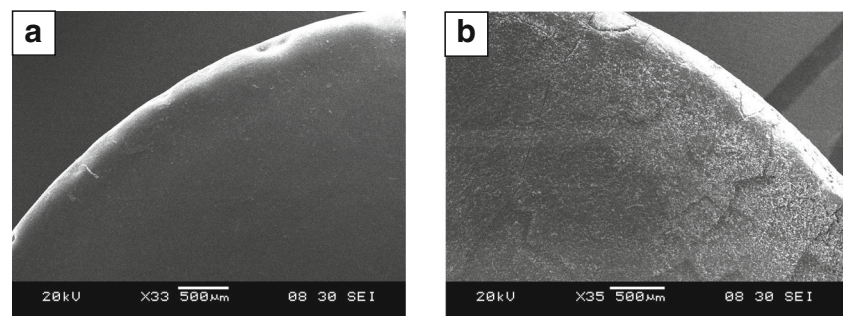
SMEC-SDs signified solubilisation of Cur irrespective of the polymer (Fig. 4). The XRD data (Fig. 5) correlated well with the DSC results. While typical Cur diffraction peaks were observed in the diffractograms of Cur and Cur SD (KSM0), the peaks were absent in Cur SMEC-SDs (KSM20) confirming that Cur was either in solubilised or amorphous form. The role of SMEC in solubilisation of Cur in the SDs was therefore confirmed. The SDs were therefore considered suitable for loading onto inert tablet cores.

### Cur SMEC-SDs Tablets

Inert tablet cores exhibited rapid disintegration in less than 2 min. By spray coating, up to 30 mg of Cur per tablet was readily loaded. Further increase in coating resulted in sticking of tablets. Furthermore as the Cur SMEC-SDs revealed tackiness within a month of storage at 40°C/75% RH a barrier coating comprising HPMC was considered. SDs coated tablets revealed hardness of 4.0–5.0 kg/cm<sup>2</sup> and complied with requirements of assay (98–100%), weight variation (250 mg  $\pm$  2%), disintegration ( $\leq$  2 min) and friability (<1%).

When dropped into aqueous media, the inert cores disintegrated rapidly to release the Cur SMEC-SDs as films (Fig. 6). The films had an approximate thickness of 100 micron, surface area 2.39 cm<sup>2</sup> and weight 66 mg which comprised ~30 mg of Cur. Considering that up to 30% w/w of

**Fig. 7** Scanning electron micrographs of (a) Cur SMEC-SDs tablets (KSM20) and (b) Cur SDs tablet (KSM0).



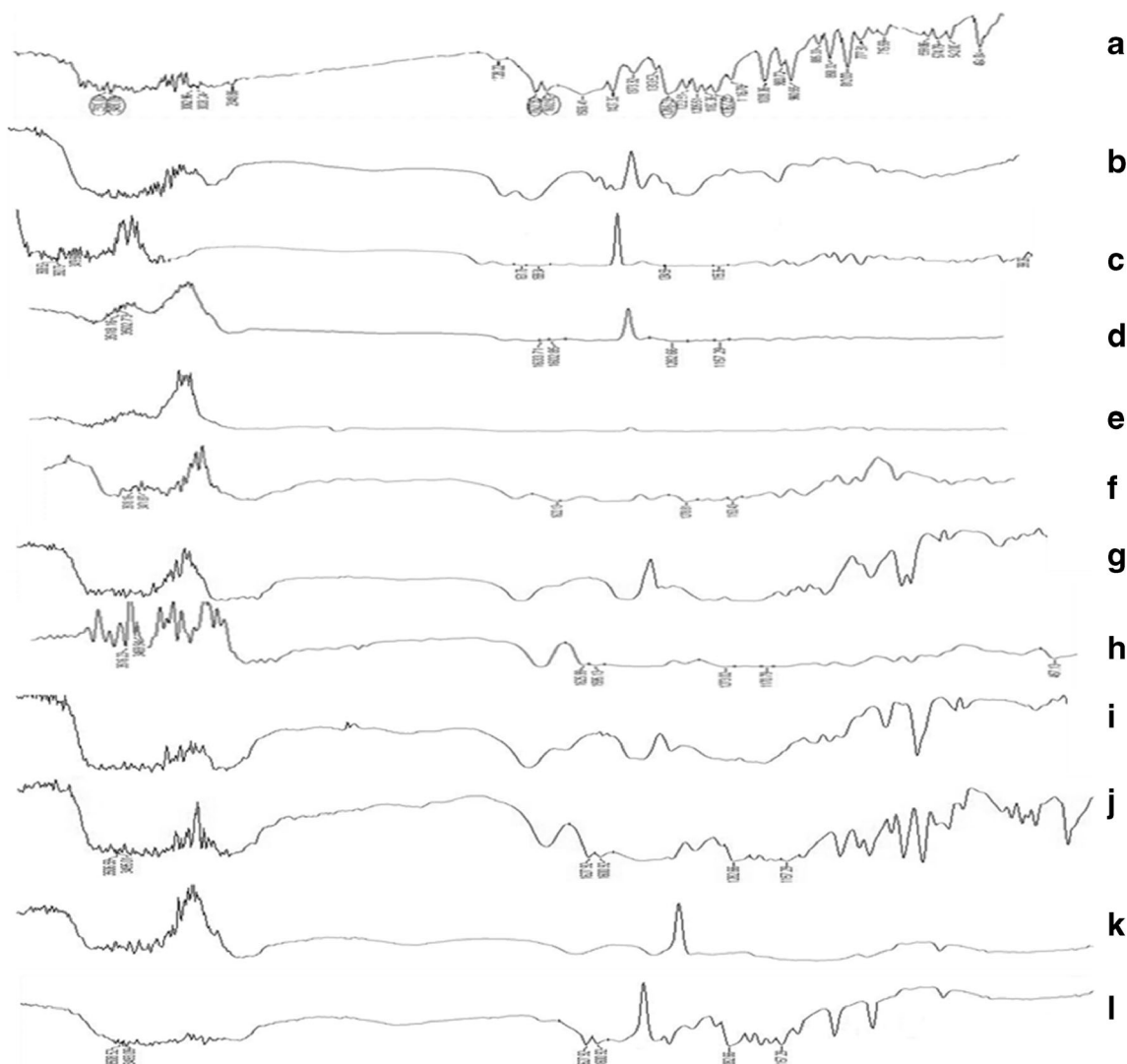


**Fig. 8** FTIR spectra of (a) Plain Cur (b) KVA (c) KVA Cur SDs (KSM0) (d) KVA Cur SMEC-SDs (KSM20) (e) HPMC (f) HPMC Cur SMEC-SDs (HSM20) (g) Eudragit EPO (h) Eudragit EPO Cur SMEC-SDs (EPSM20) (i) Soluplus (j) Soluplus Cur SMEC-SDs (SSM20) (k) Eudragit RLPO (l) Eudragit RLPO Cur SMEC-SDs (RLSM20).

drugs are reported incorporated in oral films, (24) our advanced third generation SD enabled an abnormally high drug loading of 45%. Furthermore quick dissolution of the SDs

facilitated rapid release of Cur. Cur SDs revealed slower dissolution. More importantly microemulsion formation exhibited by the Cur SMEC-SDs, with average globule size 110 nm

**Fig. 9** *In vitro* release in simulated gastric fluid (SGF) pH 1.2 (a) Effect of polymer (b) Effect of SMEC concentration.

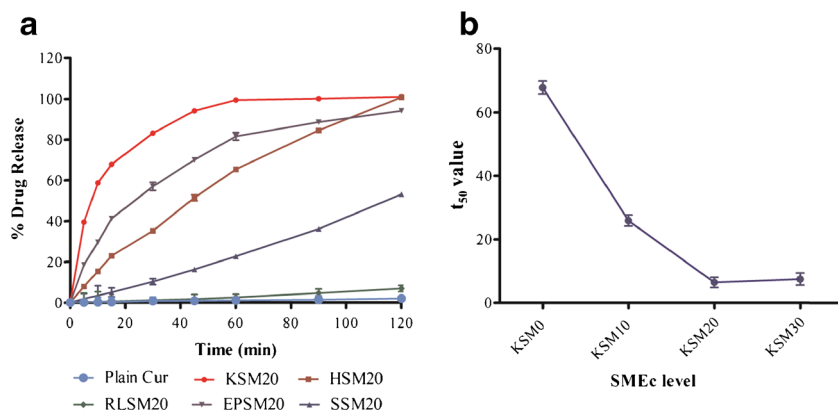




**Table II** Results of Mathematical Models after Curve Fitting *In Vitro* Drug Release Data

Formulations	R <sup>2</sup> Values for mathematical models					
	First order	Zero order	Higuchi	Hixen Crowel	Korsmeyer Pepas	n value
KSM20	0.996	0.819	0.911	0.903	0.903	0.489
EPSM20	0.989	0.927	0.979	0.952	0.975	0.481
HSM20	0.905	0.99	0.997	0.925	0.917	0.795

and PDI 0.243 also confirmed by observing the filtered solutions through an optical polarizer suggested a possible role of SMEC also in bioenhancement.

### Scanning Electron Microscopy

SEM photographs of Cur SMEC-SD (KSM20) revealed smooth, continuous, homogenous and uniform films with no evidence of crystallization of Cur, even at the end of 6 months (Fig. 7a). In the Cur SD (KSM0) crystals of Cur were clearly evident. Further the film also revealed cracks (Fig. 7b). This further substantiated the role of SMEC in advanced third generation SDs and correspondingly as crystallization inhibitor which impart physical stability.

### Contact Angle Measurement

While Cur SD (KSM0) revealed a very high contact angle of 129°, all the Cur SMEC-SDs revealed significant decrease in contact angle, attributed to the high hydrophilicity and surface active property of SMEC. The contact angle was however significantly influenced by the polymer in the SD, as seen from the values; Eudragit RLPO (27°), soluplus (24°), Eudragit EPO (15°), HPMC (14°) and KVA revealing the lowest contact angle of 7°. These differences are attributed

**Table III** Stability Data of Cur SMEC-SDs (KSM20) (mean ± S.D.; n = 3)

Sampling time	Globule size (nm)	Assay (%)	T <sub>50</sub> (min)	F2Value
Initial	102.56 ± 4.3	99.79 ± 1.22	6.45	Reference
30°C/65%RH				
1 month	112.20 ± 4.3	99.05 ± 2.26	6.35	64.25
3 month	108.25 ± 0.3	98.76 ± 2.45	6.58	59.84
6 month	115.10 ± 0.4	98.88 ± 4.27	6.80	61.23
12 months	112.50 ± 0.3	99.12 ± 3.43	7.19	62.00
45°C/75%RH				
1 month	107.51 ± 0.3	99.20 ± 2.66	6.70	67.21
3 month	117.41 ± 0.2	98.85 ± 5.31	7.11	61.22
6 month	118.63 ± 0.2	98.81 ± 0.68	6.98	63.52

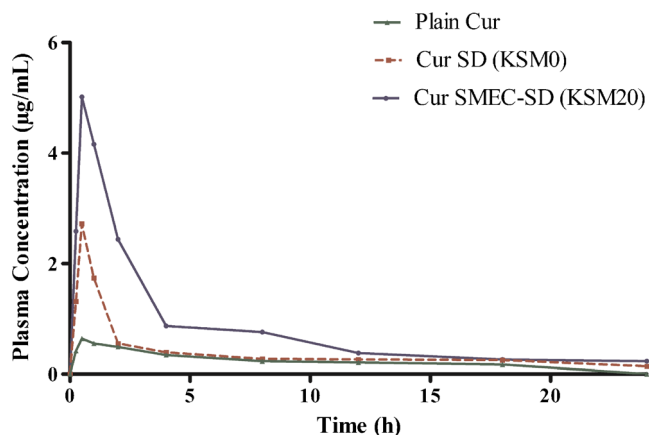
**Table IV** Pharmacokinetic Parameters after Oral Administration of Cur Formulations

Parameters	Plain Cur	KSM0 (Cur SDs)	KSM20 (Cur SMEC-SDs)
C <sub>max</sub> (μg/ml)	0.64	2.74	5.02
T <sub>max</sub> (h)	0.5	0.5	0.5
T <sub>1/2</sub> (h)	11.45	13.26	9.5
AUC <sub>0-t</sub> (h*μg/mL)	4.989	8.95	19.05
AUC <sub>0-∞</sub> (h*μg/mL)	7.79	11.55	22.21
Relative bioavailability (%)	–	216.15	413.82

to the hydrophilic nature of the polymers and the interactions of SMEC with the polymers as elucidated by FTIR.

### Fourier Transform Infrared (FTIR) Spectral Study

The infrared spectrum of Cur (Fig. 8) exhibited an O-H stretching at 3490 and 3510 cm<sup>-1</sup>. Characteristic peaks at 1627 and 1286 cm<sup>-1</sup> can be assigned to (C=C) and enol (C-O). The signature peaks at 1602 cm<sup>-1</sup> found in native Cur was due to aromatic C=C double bonds. The prominent peak at 1162 cm<sup>-1</sup> was assigned to (C-O-C) of the phenyl group mixed with methoxy group. The peaks at the same wave number in batches with KVA (KSM20), HPMC (HSM20) and Eudragit EPO (EPSM20) as polymer were very weak with sharply decreased IR absorption strength of these peaks. This is a clear indication of intramolecular or intermolecular interactions. However peaks of batches with soluplus (SSM20) and Eudragit RLPO (RLSM20) were sharp with significant intensity indicating less interaction between the Cur and carriers. The wider shape and decreased intensity of peak at 1286 cm<sup>-1</sup> can be explained by formation of hydrogen bonding between phenolic hydroxyl in Cur and the carbonyl group of KVA. Additional hydrogen bonding may

**Fig. 10** Plasma concentration vs. time profiles after oral administration of Cur formulations All values reported are mean ± SD (n = 6).

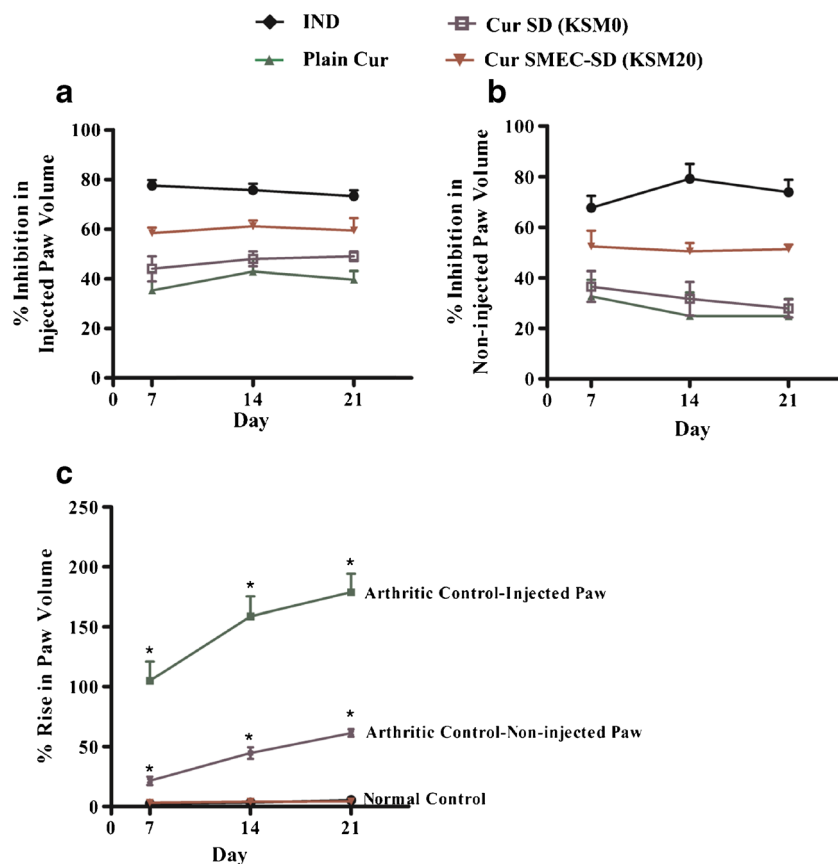
be possible between enol group (C-O) of Cur and carbonyl group of KVA. In the presence of SMEC (KSM20), figure D indicates that Cur characteristic peak at 1627 and 3510  $\text{cm}^{-1}$  almost disappeared, indicating stronger interaction of Cur with carrier KVA. Absence of carbonyl group peak at 1728  $\text{cm}^{-1}$  in figure D indicates extensive hydrogen bonding in presence of SMEC. Reduced intensity or disappearance of peaks of Cur indicated interaction with carriers, possibly through hydrogen bonds resulting due to Cur dissolved in the SMEC. Increased hydrogen bonding due to solubilisation of drug in SMEDDS is well reported (25). In KSM20 formulation a shift of peak from 3490 to 3502  $\text{cm}^{-1}$ , indicated hydrogen bonding was enhanced (26).

### In-Vitro Drug Release

Among the SDs exceptionally rapid release was observed with KVA as polymer (KSM20) with very low  $t_{50\%}$  6.45 min and  $t_{90\%}$  28.45 min. Significantly slower release was seen with all other polymers and was in the order of EPO > HPMC > Soluplus (Fig. 9). Surprisingly with Eudragit RLPO despite the high hydrophilicity reflected by the low contact angle, no release was observed even at two hours.  $t_{50\%}$  observed in order KVA < EPO < HPMC < Soluplus is attributed to the viscosity of the polymer solutions which is related to the molecular weight

of the polymers; KVA (45000 g/mol), Eudragit EPO (57000 g/mol), HPMC (100000 g/mol) and soluplus (140000 g/mol). Greater the molecular weight, higher the viscosity and slower the release.(27). A decrease in SMEC concentration (KSM10) resulted in significant increase in  $t_{50\%}$ , but increase to 30% (KSM30) exhibited no significant change in dissolution profile (F2 value 71.24) suggesting 20% SMEC as optimal. However the Cur SD revealed significantly slower dissolution with a very high  $t_{50\%}$  of greater than 60 min. Further the high aqueous solubility of KVA coupled with the hydrophilicity and surface active property of SMEC enabled remarkably rapid dissolution of Cur from the advanced third generation SDs. Drug release from the Cur SMEC-SDs was fitted to different dissolution kinetic models i.e. First-order, Zero order, Higuchi, Hixson-Crowell and Korsmeyer-Peppas (Table II). It was found that KVA and Eudragit EPO SMEC-SDs which displayed rapid dissolution exhibited first order kinetics while HPMC exhibited Higuchi kinetics. The observed 'n' values for release profile of formulation HSM20 fall in between 0.50 and 0.89 indicated anomalous release behavior coupled with diffusion and erosion. The release exponents for formulation KSM20 and EPSM20 are less than 0.5 indicating quasi fickian diffusion mechanism of drug release. Formulations of Soluplus

**Fig. 11** Effect of the IND, Plain Cur, Cur SD (KSM0) and Cur SMEC-SD (KSM20) on paw volume in Freund's Complete Adjuvant induced arthritis in rats.



and Eudragit RLPO exhibited significantly low release and hence were not assessed. All Cur SMEC-SDs revealed microemulsion formation in dissolution media with globule size in the range of 100–115 nm and PDI < 0.3.

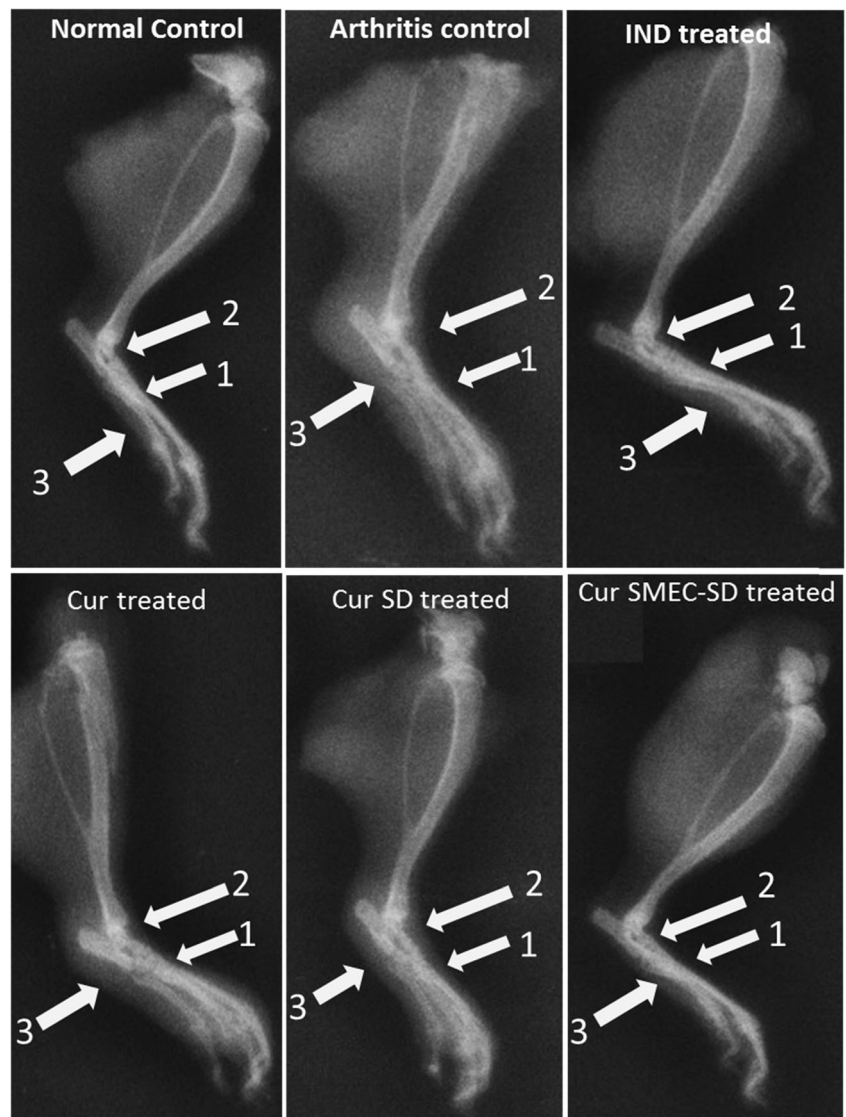
### Stability Studies

The stability data is summarized in Table III. The formulation KSM20 exhibited good stability with no change in hardness, friability and weight variation. Drug content was greater than 98% even after storage at  $40^{\circ}\text{C} \pm 2^{\circ}\text{C}$ ,  $75 \pm 5\%$  RH for 6 months. Further no significant difference in drug release ( $F_2 > 50$ ) and globule size in microemulsion range suggested good stability.

### Pharmacokinetic Study

All the formulations revealed a comparable  $t_{\text{max}}$  of 0.5 h (Table IV). Nevertheless the significant differences were seen in the  $C_{\text{max}}$ . The Cur SMEC-SDs (KSM20) revealed a high  $C_{\text{max}}$  of  $5.02 \mu\text{g}/\text{mL}$ . Cur SDs (KSM0) revealed a  $C_{\text{max}}$  of  $2.74 \mu\text{g}/\text{mL}$  while Cur revealed a very low  $C_{\text{max}}$  of  $0.64 \mu\text{g}/\text{mL}$  (Fig. 10). Bioenhancement of  $\sim 200\%$  compared to Cur was achieved with the KSM0 is attributed to KSM0 being a second generation SD. Nevertheless the bioenhancement of  $\sim 400\%$  seen with Cur SMEC-SD which was two fold higher than even KSM0 confirmed the superior role of the advanced third generation SD in bioenhancement. It is evident from the table that decrease in half life which is attributed to relative instability of curcumin is also associated with decrease in MRT. Decrease in half life and MRT could be related to

**Fig. 12** Radiographic analysis of left hind paws (injected) of rats on day 21. Arrows represent 1 = Metatarsal bones, 2 = Joint space, 3 = Soft tissue around the joints.





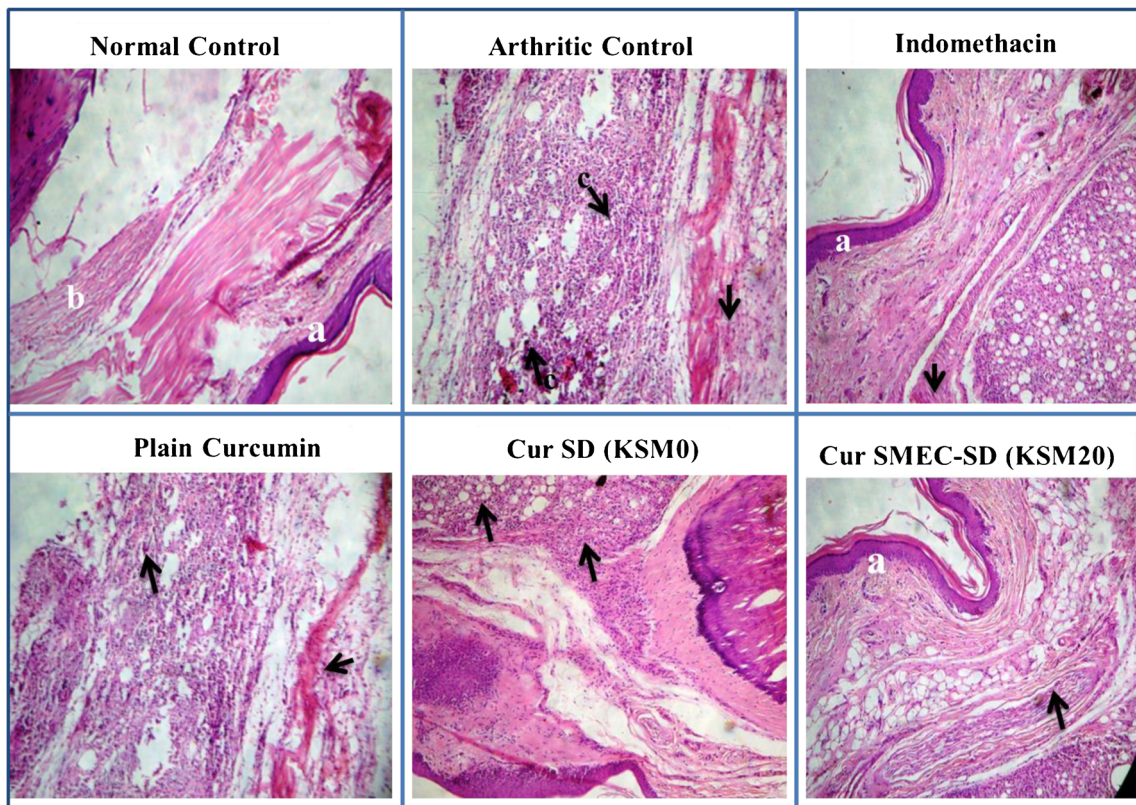


**Fig. 13** Histopathology of synovial joints of adjuvant injected paw. 'a' indicate the epidermis lined by stratified squamous epithelium and 'b' represents the dermis comprised of fibrocollagenous stroma with adnexal structures. Arrow indicates dense lymphohistiocytic and mononuclear inflammatory infiltration along with scattered epithelioid cells.

significantly higher plasma concentration of Cur from SMEC-SDs (KSM20) resulting in greater degradation.

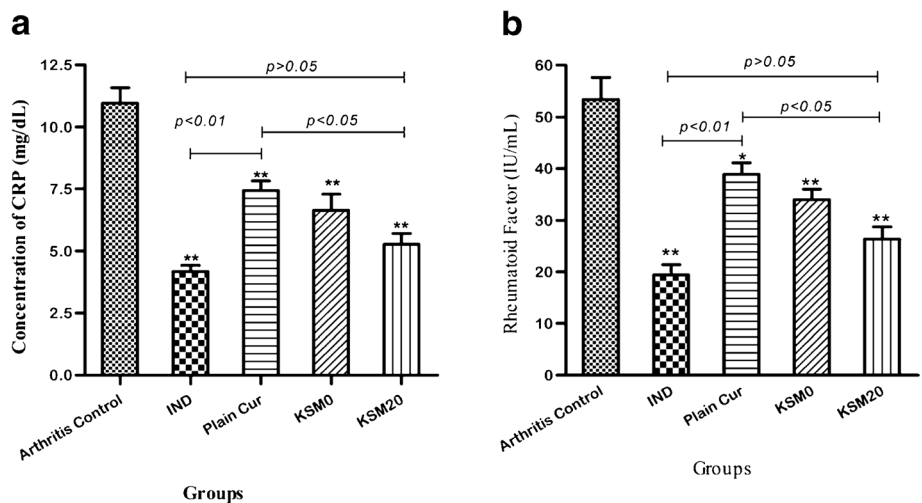
The remarkably high bioavailability seen with KSM20 is attributed to the combined effect of enhanced surface area of the SD film coupled with SMEC enabled rapid dissolution of Cur from the SDs with the microemulsion formed *in situ*, as confirmed in the *in vitro* release study, also aiding bioenhancement.

**Anti-Arthritic Activity**

*Arthritis Assessment*

The anti-inflammatory property of Cur is well established and the application of Cur as an antiarthritic is demonstrated (28). RA is a devastating chronic illness characterized by non-specific inflammation of peripheral joints, destruction of

**Fig. 14** Effect of chronic treatment in CFA-injected arthritic rats on levels of (a) CRP; (b) RF.



\*p<0.05 and \*\*p<0.01 when compared with Arthritis control

**Table V** Changes in Body Weight, Organ Weights and Hematological Parameters

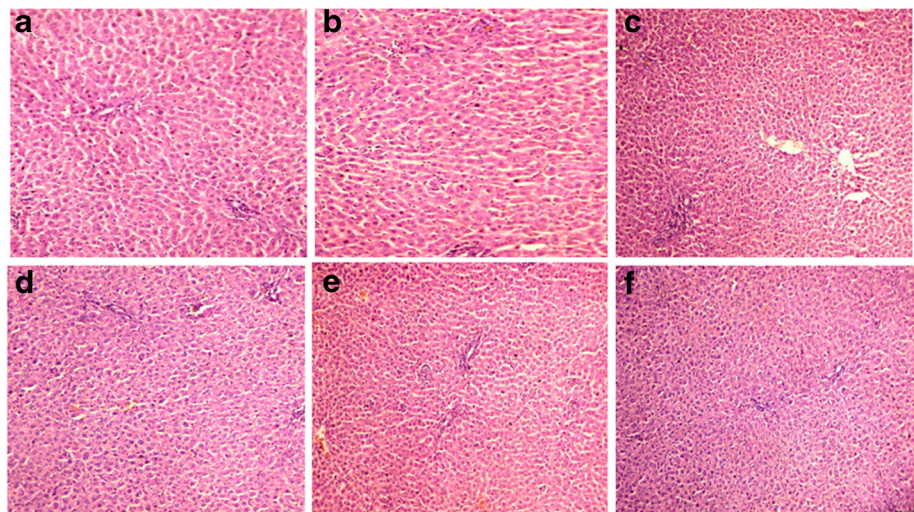
Groups	% Body weight gain (Day 21)	Spleen weight (g/100 gm body weight)	Thymus weight (g/100 gm body weight)	RBC ( $\times 10^6 \text{ mm}^3$ )	WBC ( $\times 10^6 \text{ mm}^3$ )	Hb (mg%)
Normal Control	18.7 $\pm$ 1.6	0.404 $\pm$ 0.03	0.126 $\pm$ 0.03	6.8 $\pm$ 0.5	7.9 $\pm$ 0.3	13.7 $\pm$ 0.6
Arthritis Control	8.8 $\pm$ 0.6***	0.565 $\pm$ 0.03***	0.082 $\pm$ 0.05*	3.9 $\pm$ 0.2**	13.3 $\pm$ 0.4***	7.8 $\pm$ 0.3***
INDO	17.0 $\pm$ 1.2 <sup>c, #</sup>	0.411 $\pm$ 0.021 <sup>c</sup>	0.124 $\pm$ 0.06 <sup>a</sup>	4.1 $\pm$ 0.4	7.8 $\pm$ 0.5 <sup>c</sup>	8.5 $\pm$ 0.7
Plain Cur	12.9 $\pm$ 0.8 <sup>a</sup>	0.462 $\pm$ 0.02 <sup>a</sup>	0.109 $\pm$ 1.0	5.2 $\pm$ 0.5	9.4 $\pm$ 0.4 <sup>c</sup>	11.9 $\pm$ 0.9 <sup>b</sup>
KSM0	14.5 $\pm$ 0.6 <sup>b</sup>	0.366 $\pm$ 0.02 <sup>b</sup>	0.101 $\pm$ 0.08 <sup>b</sup>	5.8 $\pm$ 0.4	9.8 $\pm$ 0.2	12.1 $\pm$ 0.8
KSM20	17.5 $\pm$ 1.3 <sup>c, #</sup>	0.394 $\pm$ 0.01 <sup>c</sup>	0.128 $\pm$ 0.023 <sup>a</sup>	6.1 $\pm$ 0.5 <sup>a</sup>	8.4 $\pm$ 0.5 <sup>c</sup>	12.6 $\pm$ 0.9 <sup>c</sup>

articular tissues and deformities in joints and requires chronic treatment (29). The profound morbidity associated with RA coupled with the side effects associated with conventional therapy, seriously affects quality of life and adversely affects patient compliance. The search for an effective yet safer less toxic alternative therapy for RA continues even today. Our objective was to evaluate Cur SMEC-SD (KSM20) for its potential in RA therapy as one such promising alternative.

The CFA control group (arthritic control) exhibited a continuous increase in the injected paw volume. The increase, although significantly lower, was also seen in the non-injected paw volume. The initial rapid swelling of  $\sim 100\%$  seen in injected paw at day 7 is attributed to edema and soft-tissue thickening caused by the irritant effect of the adjuvant at the injection site. The continued swelling from day 7–21 is due to onset of late-phase arthritis generally triggered by immunological events (30). The % inhibition in paw volume after various treatments is depicted in Fig. 11. In the injected paw Cur SMEC-SD (KSM20) treatment showed significantly higher inhibition of paw volume than plain Cur and Cur SD (KSM0) ( $p < 0.05$ ) indicating enhanced efficacy of Cur. Furthermore, an

inhibition of  $\sim 82\%$  of that seen with the IND treatment group suggests great promise of Cur SMEC-SD (KSM20). An increase in the non-injected paw volume suggested secondary arthritic lesions, a manifestation of cell-mediated immunity (31). Suppression of such secondary lesions is an indicator of immunomodulatory action. As seen with the injected paw, Cur SMEC-SD revealed significant inhibition in the non-injected paw volume compared to Cur and Cur SD ( $p < 0.05$ ), and an effect which was  $\sim 70\%$  in comparison to the IND group (Fig. 11). X-ray radiographs (Fig. 12) of injected paws on day 21 showed definite joint space narrowing between tibia and tarsal bone, severe soft tissue swelling and edema and enlargement of metatarsal bones in CFA treated rats. While the Cur SMEC-SD (KSM20) and IND groups exhibited significant and comparable inhibition of soft tissues swelling and bone enlargement, this was not evident with plain Cur and Cur SD (KSM0) groups. This enhanced antiedematous effect was also confirmed by histopathological analysis of the synovial joints of the injected paws of Cur SMEC-SD and IND treated rats which revealed significant

**Fig. 15** Haematoxylin and eosin (H&E)-stained longitudinal section of liver of (a) saline treated rats (normal rats), (b) Arthritic Control, (c) IND, (d) Plain Cur, (e) Cur SD (KSM0), and (f) Cur SMEC-SD (KSM20).





inhibition of inflammatory tissue alteration (Fig. 13). Superior antiarthritic activity of Cur SMEC SD compared to Cur and quite comparable to IND was therefore suggested.

CFA induced arthritis also mimics human rheumatoid arthritis in immunological and biochemical features (32,33). These involve increase in macrophage and WBC generation resulting in the upregulation of different cytokines (interleukines and Tumor necrosis factor), NF- $\kappa$ B, monocyte chemotactic protein-1 (MCP-1) which results in an increase in spleen weight and decrease in thymus weight. These upregulations reorchestrate the pattern of gene expression in hepatocyte with increase in levels of the acute phase blood protein, CRP (34). B-cell activation also results in upregulation of RF, an antibody, directed against Fc portion of IgG to form immune complexes, which is a prominent immunological abnormality involved in pathogenesis of RA (35). Hence CRP, RF, WBC and organ weights were evaluated as immunopathological marker of RA. The arthritic control rats exhibited very high CRP, RF and WBC levels along with increase in spleen and decrease in thymus weight, confirming successful development of adjuvant induced arthritis in rats (Fig. 14, Table V). No significant changes in body weight, weight of spleen and thymus was observed in IND and Cur SMEC-SD group while a decrease body weight in thymus weight and increase in spleen weight seen with Cur and Cur SD. As IND is a recommended drug for RA therapy this finding validates the promise of the Cur SMEC SD for RA therapy. However the IND group exhibited significant decrease in RBC count and hemoglobin percentage (Table V). Such decrease has also been reported with methotrexate and cyclosporine used for treatment of RA, and is indicator of hematological toxicity (22). In contrast Cur SMEC-SD did not affect RBC count and hemoglobin percentage confirming its safety. Liver toxicity is also considered as a serious limitation of IND therapy which is often a prime cause of patient noncompliance. Histopathology of liver revealed marked lesions (Grade 4) in the IND treated group which indicated significant liver toxicity. No apparent histopathological changes were seen with Cur SMEC-SD indicating safety (Fig. 15).

The importance of bioenhanced Cur is spelled out clearly in our study wherein Cur SMEC-SD (KSM20) which revealed relative bioavailability of over 400% related to Cur demonstrated an anti-arthritic efficacy nearly comparable with an IND and comparable efficacy with respect to inhibition of CRP and RA with the desired advantage of enhanced safety compared to IND. The study therefore proposes Cur SMEC-SD as an efficacious and promising alternative for treatment of rheumatoid arthritis.

## CONCLUSION

The advanced third generation SDs of Cur as films presents an innovative approach in SD technology. The successful application of this technology is demonstrated for curcumin a nutraceutical challenged by poor bioavailability. The simple technology proposed for designing the advanced third generation SDs as film, also suggests scalability. More importantly it provides a bioenhanced curcumin formulation which could be explored for manifold therapeutic applications of Cur.

## ACKNOWLEDGMENTS AND DISCLOSURES

Authors are thankful to Phoenix Pharmaceuticals LLC, USA for providing fellowship to Prashant Mande.

Phoenix Pharmaceuticals LLC, USA

## REFERENCES

1. Anand P, Kunnumakkara AB, Newman RA, Aggarwal BB. Bioavailability of curcumin: problems and promises. *Mol Pharm.* 2007;4(6):807–18.
2. Seo S-W, Han H-K, Chun M-K, Choi H-K. Preparation and pharmacokinetic evaluation of curcumin solid dispersion using Solutol® HS15 as a carrier. *Int J Pharm.* 2012;424(1):18–25.
3. Maiti K, Mukherjee K, Gantait A, Saha BP, Mukherjee PK. Curcumin–phospholipid complex: preparation, therapeutic evaluation and pharmacokinetic study in rats. *Int J Pharm.* 2007;330(1): 155–63.
4. Gong C, Deng S, Wu Q, Xiang M, Wei X, Li L, *et al.* Improving antiangiogenesis and anti-tumor activity of curcumin by biodegradable polymeric micelles. *Biomaterials.* 2013;34(4):1413–32.
5. Bergonzi M, Hamdouch R, Mazzacuvva F, Isacchi B, Bilia A. Optimization, characterization and in vitro evaluation of curcumin microemulsions. *LWT-Food Sci Technol.* 2014;59(1):148–55.
6. Kakkar V, Mishra AK, Chuttani K, Kaur IP. Proof of concept studies to confirm the delivery of curcumin loaded solid lipid nanoparticles (C-SLNs) to brain. *Int J Pharm.* 2013;448(2):354–9.
7. Nguyen TN-G, Tran PH-L, Van Tran T, Van Vo T, Truong-Dinh Tran T. Development of a modified–solid dispersion in an uncommon approach of melting method facilitating properties of a swellable polymer to enhance drug dissolution. *Int J Pharm.* 2015;484(1):228–34.
8. Li B, Konecke S, Wegiel LA, Taylor LS, Edgar KJ. Both solubility and chemical stability of curcumin are enhanced by solid dispersion in cellulose derivative matrices. *Carbohydr Polym.* 2013;98(1): 1108–16.
9. Vasconcelos T, Sarmento B, Costa P. Solid dispersions as strategy to improve oral bioavailability of poor water soluble drugs. *Drug Discov Today.* 2007;12(23):1068–75.
10. Vo CL-N, Park C, Lee B-J. Current trends and future perspectives of solid dispersions containing poorly water-soluble drugs. *Eur J Pharm Biopharm.* 2013;85(3):799–813.
11. Won D-H, Kim M-S, Lee S, Park J-S, Hwang S-J. Improved physicochemical characteristics of felodipine solid dispersion particles by supercritical anti-solvent precipitation process. *Int J Pharm.* 2005;301(1):199–208.
12. Dannenfels RM, He H, Joshi Y, Bateman S, Serajuddin A. Development of clinical dosage forms for a poorly water soluble

- drug I: application of polyethylene glycol–polysorbate 80 solid dispersion carrier system. *J Pharm Sci.* 2004;93(5):1165–75.
13. Zaki RM, Ali AA, El Menshawi SF, Bary AA. Effect of binary and ternary solid dispersions prepared by fusion method on the dissolution of poorly water soluble diacerein. *Int J Drug Delivery.* 2013;5(1):99.
  14. Yu D-G, Yang J-M, Branford-White C, Lu P, Zhang L, Zhu L-M. Third generation solid dispersions of ferulic acid in electrospun composite nanofibers. *Int J Pharm.* 2010;400(1):158–64.
  15. Pouton CW. Formulation of poorly water-soluble drugs for oral administration: physicochemical and physiological issues and the lipid formulation classification system. *Eur J Pharm Sci.* 2006;29(3):278–87.
  16. Heo M-Y, Piao Z-Z, Kim T-W, Cao Q-R, Kim A, Lee B-J. Effect of solubilizing and microemulsifying excipients in polyethylene glycol 6000 solid dispersion on enhanced dissolution and bioavailability of ketoconazole. *Arch Pharm Res.* 2005;28(5):604–11.
  17. Beg S, Sharma G, Thanki K, Jain S, Katare O, Singh B. Positively charged self-nanoemulsifying oily formulations of olmesartan medoxomil: systematic development, in vitro, ex vivo and in vivo evaluation. *Int J Pharm.* 2015;493(1):466–82.
  18. Boateng JS, Matthews KH, Auffret AD, Humphrey MJ, Stevens HN, Eccleston GM. In vitro drug release studies of polymeric freeze-dried wafers and solvent-cast films using paracetamol as a model soluble drug. *Int J Pharm.* 2009;378(1):66–72.
  19. Nascimento A, Neto EB, Moura M, Dantas TC, Neto AD. Wettability of paraffin surfaces by nonionic surfactants: Evaluation of surface roughness and nonylphenol ethoxylation degree. *Colloids and Surfaces A: Physicochemical and Engineering Aspects.* 2014.
  20. Setthacheewakul S, Mahattanadul S, Phadoongsombut N, Pichayakorn W, Wiwattanapatapee R. Development and evaluation of self-microemulsifying liquid and pellet formulations of curcumin, and absorption studies in rats. *Eur J Pharm Biopharm.* 2010;76(3):475–85.
  21. Chopra S, Venkatesan N, Betageri GV. Formulation of lipid bearing pellets as a delivery system for poorly soluble drugs. *Int J Pharm.* 2013;446(1):136–44.
  22. Banji D, Pinnapureddy J, Banji OJ, Saidulu A, Hayath MS. Synergistic activity of curcumin with methotrexate in ameliorating Freund's complete adjuvant induced arthritis with reduced hepatotoxicity in experimental animals. *Eur J Pharmacol.* 2011;668(1):293–8.
  23. Zhang L, Zhu W, Yang C, Guo H, Yu A, Ji J, *et al.* A novel folate-modified self-microemulsifying drug delivery system of curcumin for colon targeting. *Int J Nanomedicine.* 2012;7:151.
  24. Dixit R, Puthli S. Oral strip technology: overview and future potential. *J Control Release.* 2009;139(2):94–107.
  25. Hu X, Lin C, Chen D, Zhang J, Liu Z, Wu W, *et al.* Sirolimus solid self-microemulsifying pellets: formulation development, characterization and bioavailability evaluation. *Int J Pharm.* 2012;438(1):123–33.
  26. Mohanty C, Sahoo SK. The in vitro stability and in vivo pharmacokinetics of curcumin prepared as an aqueous nanoparticulate formulation. *Biomaterials.* 2010;31(25):6597–611.
  27. Zeng Z, Sun L, Xue W, Yin N, Zhu W. Relationship of intrinsic viscosity to molecular weight for poly(1, 4-butylene adipate). *Polym Test.* 2010;29(1):66–71.
  28. Moon D-O, Kim M-O, Choi YH, Park Y-M, Kim G-Y. Curcumin attenuates inflammatory response in IL-1 $\beta$ -induced human synovial fibroblasts and collagen-induced arthritis in mouse model. *Int Immunopharmacol.* 2010;10(5):605–10.
  29. Obiri DD, Osafo N, Ayande PG, Antwi AO. *Xylopi*a aethiopica (Annonaceae) fruit extract suppresses Freund's adjuvant-induced arthritis in Sprague–Dawley rats. *J Ethnopharmacol.* 2014;152(3):522–31.
  30. Ward JR, Cloud RS. Comparative effect of antirheumatic drugs on adjuvant-induced polyarthritis in rats. *J Pharmacol Exp Ther.* 1966;152(1):116–21.
  31. Bani S, Kaul A, Khan B, Gupta VK, Satti NK, Suri KA, *et al.* Anti-arthritic activity of a biopolymeric fraction from *Euphorbia tirucalli*. *J Ethnopharmacol.* 2007;110(1):92–8.
  32. Behar SM, Porcelli SA. Mechanisms of autoimmune disease induction. *Arthritis Rheumatism.* 1995;38(4):458–76.
  33. Kumar DA, Manikandan P, Sumitra M, Raju KVN, Gayathri C, Arutselvan N, *et al.* A novel peptide derivative exhibits antiinflammatory and antioxidant activity in adjuvant induced arthritis in rats. *Mol Cell Biochem.* 2002;229(1–2):9–17.
  34. Ridker P. Should statin therapy be considered for patients with elevated C-reactive protein? The need for a definitive clinical trial. *Eur Heart J.* 2001;23(22):2135–7.
  35. Bauerova K, Acquaviva A, Ponist S, Gardi C, Vecchio D, Drafi F, *et al.* Markers of inflammation and oxidative stress studied in adjuvant-induced arthritis in the rat on systemic and local level affected by pinosylvlin and methotrexate and their combination. *Autoimmunity.* 2015;48(1):46–56.